Holotomography: Quantitative phase tomography with micrometer resolution using hard synchrotron radiation x rays

P. Cloetens,[a] W. Ludwig, and J. Baruchel
European Synchrotron Radiation Facility (ESRF), F-38043 Grenoble, France

D. Van Dyck and J. Van Landuyt
EMAT, University of Antwerp (RUCA), B-2020 Antwerp, Belgium

J. P. Guigay[b] and M. Schlenker
Laboratoire Louis Néel du CNRS, F-38042 Grenoble, France

(Received 28 May 1999; accepted for publication 8 September 1999)

Because the refractive index for hard x rays is slightly different from unity, the optical *phase* of a beam is affected by transmission through an object. Phase images can be obtained with extreme instrumental simplicity by simple propagation provided the beam is coherent. But, unlike absorption, the phase is not simply related to image brightness. A holographic reconstruction procedure combining images taken at different distances from the specimen was developed. It results in quantitative phase mapping and, through association with three-dimensional reconstruction, in holotomography, the complete three-dimensional mapping of the density in a sample. This tool in the characterization of materials at the micrometer scale is uniquely suited to samples with low absorption contrast and radiation-sensitive systems. © *1999 American Institute of Physics.* [S0003-6951(99)03145-9]

X-ray *phase* imaging was first attempted[1] and developed using Bonse–Hart type x-ray interferometers,[2] and extended to phase tomography[3] in spite of its considerable instrumental difficulty and limited spatial resolution. Fresnel diffraction, the analogue of the focus variation method of electron microscopy, provides excellent phase images very simply, provided the beam is spatially coherent.[4,5] As the sample-detector distance D is increased, the effect of a pure phase feature changes from no contrast at zero distance to the edge-detection regime, in which phase jumps associated with discontinuities are delineated by fine fringes, and into a conspicuous Fresnel fringe system. Qualitative tomography can be performed in the edge-detection mode[6] using the reconstruction algorithm of absorption tomography. However, the information on the phase is contained in the fringes, and schemes must be devised to extract it. Some quantitative information on the low spatial frequency part can be extracted from a single hard x-ray image of a pure phase object.[7] Basically, the need for data recorded at several distances is made clear by the Talbot effect:[8,9] a periodic phase object with period a produces no contrast at distances pa^2/λ, λ being the wavelength and p an integer. Thus, Fresnel imaging at a given distance D is blind to some spatial frequencies in the phase distribution. We developed a ''holographic'' reconstruction procedure, based on a scheme proposed for high resolution electron microscopy,[10,11] to disentangle the phase map from the images. It yields an image of the sample that can be interpreted easily, and quantitative information, a prerequisite for three-dimensional imaging. The experimental setup is schematically shown on Fig. 1.

We consider for simplicity the case of a pure phase object, with transmission function $T(\mathbf{x})=\exp[i\varphi(\mathbf{x})]$. The phase $\varphi(\mathbf{x})$, relative to propagation in vacuum, at position $\mathbf{x}(x,y,0)$ in a plane perpendicular to the mean propagation direction z, right at the exit of the sample, is $\varphi(\mathbf{x})=-(2\pi/\lambda)\int\delta(x,y,z)\mathrm{d}z$, $\delta=r_c\lambda^2\rho_e/(2\pi)$ being the real part of the deviation from unity of the refractive index $n=1-\delta+i\beta$, with r_c the classical electron radius (2.8 fm), and ρ_e the electron density, corrected for dispersion if necessary. The refractive index decrement $\delta(\approx 10^{-6})$, can be two or three orders of magnitude bigger than the absorption index β.

The Fourier Transform (FT) of the intensity distribution at distance $D_m(m=1\cdots N)$ is[12]

$$\tilde{I}_m(\mathbf{f})=\delta_{\mathrm{D}}(\mathbf{f})+\tilde{R}_m(\mathbf{f})2\sin(\pi\lambda D_m\mathbf{f}^2)\tilde{\varphi}(\mathbf{f})+\tilde{I}_{\mathrm{NL},m}(\mathbf{f}). \tag{1}$$

The FT of $\varphi(\mathbf{x})$ and of the intensity distribution $I_m(\mathbf{x})$ at distance D_m are thus linearly related provided the nonlinear term $\tilde{I}_{\mathrm{NL},m}(\mathbf{f})$ involving the superposition of different spatial frequencies is small. This will be the case in this differential phase method if[12] $|\varphi(\mathbf{s}+\lambda D_m\mathbf{f})-\varphi(\mathbf{s})|\ll 1$ for all points $\mathbf{s}$. The Dirac distribution $\delta_{\mathrm{D}}(\mathbf{f})$ corresponds to the unit mean

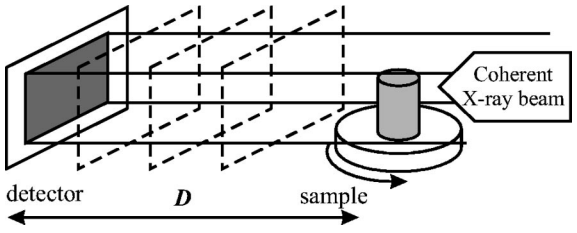

FIG. 1. Schematic drawing of the setup. Images recorded at different distances from the sample are combined to retrieve numerically the phase of the wave exiting the sample. This is repeated for a large number of angular positions of the specimen.

[a]Electronic mail: cloetens@esrf.fr
[b]Present address: ESRF, F-38043 Grenoble, France.

intensity. The multiplicative factor $\tilde{R}_m(\mathbf{f}) = \tilde{R}(\mathbf{f})\,\gamma^c(\lambda D_m \mathbf{f})$ includes the detector transfer function $\tilde{R}(\mathbf{f})$ and the degree of spatial coherence $\gamma^c(\lambda D_m \mathbf{f})$ in the object plane.[13] Using several distances obviates the blindness to some spatial frequencies, associated with zeros in the contrast factor $2\sin(\pi\lambda D_m \mathbf{f}^2)$. Also in the more general case of a nonzero amplitude modulation, images corresponding to different distances allow to solve the twin-image problem.[11] The images are combined in such a way that the relative importance of the nonlinear terms is reduced. A least-squares approach, neglecting these terms, leads to a unique initial estimate

$$H(\mathbf{f})\,\tilde{\varphi}(\mathbf{f}) = \frac{1}{N}\sum_{m=1}^{N} H_m(\mathbf{f})\,\tilde{I}_m^{\exp}(\mathbf{f}) \tag{2}$$

with

$$H_m(\mathbf{f}) = \tilde{R}_m(\mathbf{f}) \quad \sin(\pi\lambda D_m \mathbf{f}^2), \tag{3}$$

$$H(\mathbf{f}) = \frac{1}{N}\sum_{m=1}^{N} \tilde{R}_m^2(\mathbf{f}) 2\sin^2(\pi\lambda D_m \mathbf{f}^2). \tag{4}$$

This estimate is then recursively optimized[10,14] using a full description of the nonlinear image formation process. The approach is based on the Fresnel diffraction approximation and is efficiently implemented using fast FTs. The use of different distances reduces the risk of finding a local optimum or a nonunique solution.

Once the phase maps are obtained through holographic reconstruction, there is no conceptual difficulty in bringing together many maps corresponding to different orientations of the sample, and in producing the tomographic reconstruction.

We applied the combined procedure to obtain structural information about a $0.7\times0.5\times1$ mm^3 piece of polystyrene foam, an excellent approximation to a phase object for the hard ($\lambda = 0.69$ Å) x rays used, at the imaging beamline ID19 of European Synchrotron Radiation Facility. We used a charge coupled device based detector involving x-ray/visible light conversion in a transparent yttrium–aluminum–garnet:Ce screen,[15] with a pixel size of 0.95 μm. The detector transfer function was determined from its edge spread function. The degree of coherence of the beam was determined using the Talbot self-imaging effect,[9] yielding angular divergences of 1.9 and 1.2 μrad in the horizontal and vertical directions.

For each of 700 angular positions of the sample, the approximate phase map was directly retrieved using images recorded at four distances, then improved in ten recursion steps with a nonlinear least-squares method assuming no amplitude modulation. Figure 2 shows one recorded image and the reconstructed two-dimensional (2D) phase map obtained from the Fresnel diffraction patterns recorded at defocusing distances D of 0.027, 0.207, 0.505, and 0.901 m. The maximum phase modulation exceeds 2π although no separate phase unwrapping techniques were used. These techniques may, however, be necessary when the phase modulation is several times 2π. The highest accessible spatial frequency is determined by the resolution of the detector. The lowest frequencies are difficult to retrieve as they require a large propagation distance for optimum contrast. The phase map in Fig. 2(b) is a projection along the x-ray path of the electron

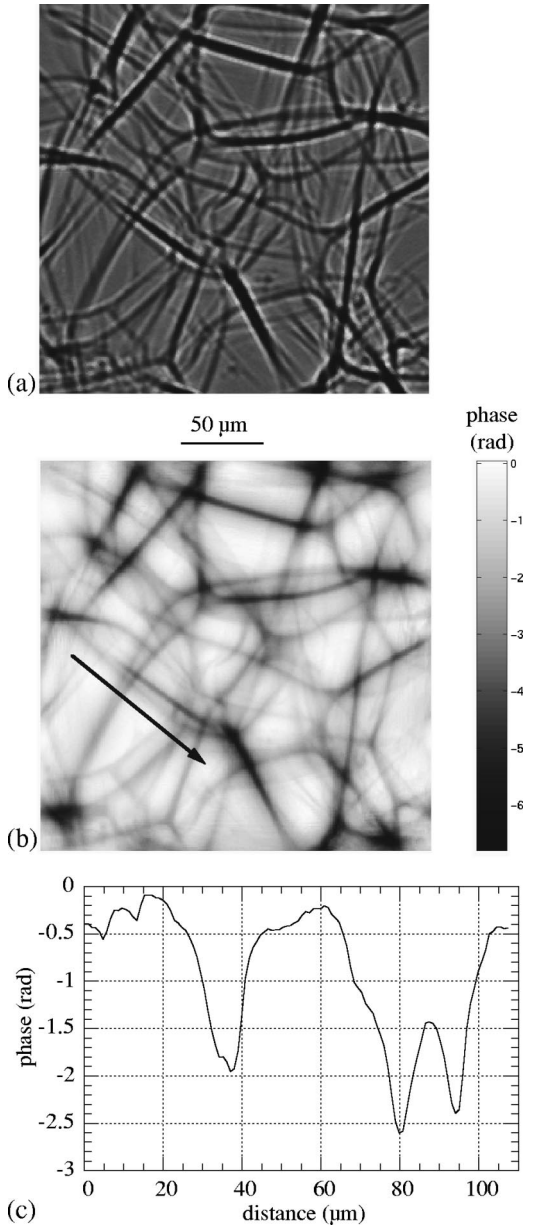

FIG. 2. (a) x-ray phase sensitive radiograph of a polystyrene foam recorded at a distance of 0.207 m. White corresponds to locally enhanced x-ray intensity. (b) Phase map reconstructed from four such Fresnel diffraction patterns at different distances from the specimen. The color bar indicates the correspondence between the gray level and the relative phase. (c) Phase profile obtained along the arrow shown in Fig. 2(b). The x-ray energy was 18 keV.

density in the sample and clearly reveals cells with sizes on the order of 100-200 μm. It is, however, not possible to unambiguously discriminate whether the linear features correspond to cell walls running almost parallel to the x-ray beam or to struts corresponding to three-wall junctions. Neither is the interconnected or closed character of the cells clearly imaged.

The 700 quantitative phase maps were the input for the tomographic reconstruction, providing the 3D distribution of the refractive index decrement, or of the electron density. Figure 3 shows a volume rendition and a slice through the reconstructed distribution. Their interpretation is straightforward and the data are well suited for further automatic processing such as binarisation or skeleton determination. The

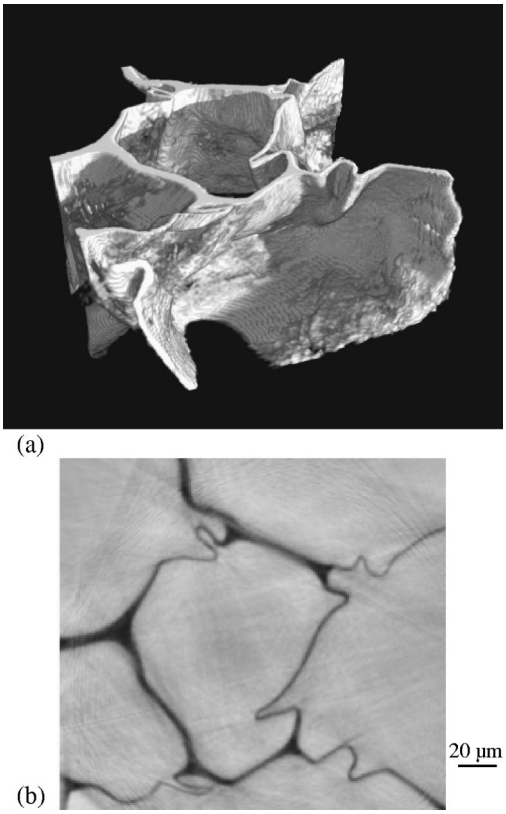

FIG. 3. (a) Volume rendition showing an enclosed foam cell. (b) Tomographic slice through the 3D distribution of the refractive index decrement in quantitative agreement with the expected electron density.

contrast is excellent. It would certainly be bad in absorption tomography, the ratio of the refractive index decrement and the absorption index δ/β being approximately 2500. The good 3D isotropic spatial resolution is due to the detector resolution but also to the holographic reconstruction disentangling the object information from the defocused images. The value of the index decrement δ in a region that apparently contains only polystyrene is $6.6\ 10^{-7}$, corresponding to a specific mass value of 0.96 g/cm^3, whereas the expected value is about 1 g/cm^3. The tomographic slice of Fig. 3(b) intersects a cell, completely enclosed by a polymer wall with conspicuous creases in its thinner parts. This complicated cell wall shape is obviously not only determined by a simple principle such as minimization of the wall area, and is related to a crushing process.

The total time to record four times 700 images was about one day (25 s/image). This value can now be reduced to less than 1 h by using a large bandwidth monochromator ($\Delta E/E \approx 10^{-2}$) instead of a monochromator based on perfect silicon crystals. The total absorbed dose in the sample is estimated to be about 60 kGy, below the threshold introducing structural modifications in wet samples.[16] Equivalent contrast could be obtained in absorption tomography by using x rays with a much lower energy of 1–2 keV, but this would entail an increase by three orders of magnitude of the dose.

This example illustrates the drastic improvement in sensitivity and resolution that hard x-ray phase radiography and tomography provide for light materials. The quantitative 3D mapping of the electron or mass density at the micrometer scale brings out important information about microstructure, opening up welcome possibilities in the nondestructive, detailed observation of systems of interest for materials science as well as for biology.

[1] M. Ando and S. Hosoya, in *Proceedings of the 6th International Conference on X-ray Optics and Microanalysis*, edited by G. Shinoda, K. Kohra, and T. Ichinokawa (University of Tokyo Press, Tokyo, 1972), pp. 63–68.
[2] U. Bonse and M. Hart, Appl. Phys. Lett. **6**, 155 (1965).
[3] A. Momose, T. Takeda, Y. Itai, and K. Hirano, Nat. Med. (N.Y.) **2**, 473 (1996).
[4] A. Snigirev, I. Snigireva, V. Kohn, S. Kuznetsov, and I. Schelokov, Rev. Sci. Instrum. **66**, 5486 (1995).
[5] P. Cloetens, R. Barrett, J. Baruchel, J. P. Guigay, and M. Schlenker, J. Phys. D **29**, 133 (1996).
[6] P. Cloetens, M. Pateyron-Salomé, J. Y. Buffière, G. Peix, J. Baruchel, F. Peyrin, and M. Schlenker, J. Appl. Phys. **81**, 5878 (1997).
[7] K. A. Nugent, T. E. Gureyev, D. F. Cookson, D. Paganin, and Z. Barnea, Phys. Rev. Lett. **77**, 2961 (1996).
[8] H. F. Talbot, Philos. Mag. **9**, 401 (1836).
[9] P. Cloetens, J. P. Guigay, C. de Martino, J. Baruchel, and M. Schlenker, Opt. Lett. **22**, 1059 (1997).
[10] W. Coene, G. Janssen, M. Op de Beeck, and D. Van Dyck, Phys. Rev. Lett. **69**, 3743 (1992).
[11] M. Op de Beeck, D. Van Dyck, and W. Coene, Ultramicroscopy **64**, 167 (1996).
[12] J. P. Guigay, Optik (Stuttgart) **49**, 121 (1977).
[13] M. Born and E. Wolf, *Principle of Optics, 6th ed.* (Pergamon, Oxford, New York, 1980).
[14] E. J. Kirkland, Ultramicroscopy **15**, 151 (1984).
[15] A. Koch, C. Raven, P. Spanne, and A. Snigirev, J. Opt. Soc. Am. A **15**, 1940 (1998).
[16] D. Sayre and H. N. Chapman, Acta Crystallogr., Sect. A: Cryst. Phys., Diffr., Theor. Gen. Crystallogr. **51**, 237 (1995).